


RESEARCH ARTICLE OPEN ACCESS

Evaluation of Glutathione T_2 in the Human Brain Using J-Difference MRS at 3 T: Multicenter Multivendor Study

Grace Choi¹ | Seungho Kim² | Ralph Noeske³ | Jason E. Moore¹ | Gang Ho Lee⁴ | Jihyun Kim⁵ | Allen T. Newton^{1,6} | Ryan K. Robison^{1,6,7} | Yongmin Chang^{8,9}  | Changho Choi^{1,6,10} 

¹Vanderbilt University Institute of Imaging Science, Vanderbilt University Medical Center, Nashville, Tennessee, USA | ²Institute of Biomedical Engineering Research, Kyungpook National University, Daegu, South Korea | ³GE HealthCare, Munich, Germany | ⁴Department of Chemistry, Kyungpook National University, Daegu, South Korea | ⁵Department of Chemistry Education, Kyungpook National University, Daegu, South Korea | ⁶Department of Radiology and Radiological Sciences, Vanderbilt University Medical Center, Nashville, Tennessee, USA | ⁷Philips, Nashville, Tennessee, USA | ⁸Department of Molecular Medicine, School of Medicine, Kyungpook National University, Daegu, South Korea | ⁹Department of Radiology, Kyungpook National University Hospital, Daegu, South Korea | ¹⁰Department of Psychiatry and Behavioral Sciences, Vanderbilt University Medical Center, Nashville, Tennessee, USA

Correspondence: Yongmin Chang (ychang@knu.ac.kr) | Changho Choi (changho.choi@vumc.org)

Received: 1 October 2024 | **Revised:** 3 December 2024 | **Accepted:** 4 December 2024

Funding: This work was supported by the National Research Foundation of Korea (Grant RS-2024-00406209) and the National Institutes of Health (Grants S10OD021771-01 and UL1TR002243).

Keywords: 3T | glutathione | human brain | J-difference MRS (MEGA) | T_2 relaxation

ABSTRACT

The need to quantify brain glutathione (GSH) accurately by J-difference spectroscopy has stimulated assessment of the TE effects on GSH edited signals at the popular field strength 3T. We performed multiple-TE J-difference MRS at two sites to evaluate the GSH T_2 relaxation and TE dependence of the GSH signal resolution. Two 10-ms spectrally selective Gaussian editing RF pulses were implemented in 3T MEGA-PRESS sequences at two sites having different vendors. The sequences were optimized, with numerical and phantom analyses, for editing of the GSH 2.95 ppm resonance. The timings of the editing pulses within the sequences were tailored for high-amplitude GSH signal production for a TE range of 58–160 ms. In vivo human brain data were collected at five TEs (58, 70, 88, 116, and 150 ms) from five subjects at each site. Following LCModel analysis of difference and edit-off spectra independently between the sites, metabolite T_2 values were estimated with mono-exponential regression of the signal estimates. Simulations and phantom data indicated that the MEGA-edited GSH peak amplitude was progressively larger with increasing TE up to 125–140 ms and the maximum amplitude was 2- to 2.5-fold greater than the amplitude at TE of 58 ms. For in vivo data, the edited GSH peak was the largest at TE of 88 ms among the five TEs. Brain GSH T_2 was measured as 88 ± 11 ms from 10 subjects, with no significant difference between the sites. The LCModel-returned correlation coefficient between GSH and co-edited *N*-acetylaspartate (NAA) multiplet was significantly smaller at short TEs than at long TEs. Our data suggest that MEGA-edited GSH signal undergoes extensive attenuation with increasing TE due to the fast T_2 relaxation, and the edited GSH signal can be well resolved at short TEs with small interferences from adjacent co-edited NAA multiplet.

Abbreviations: CRLB, Cramér–Rao lower bounds; FID, free-induction decay; FWHM, full width at half magnitude; GSH, glutathione; MEGA, Mescher–Garwood; NAA, *N*-acetylaspartate; PRESS, point-resolved spectroscopy; RF, radiofrequency; SNR, signal-to-noise ratio; SS, slice selective; tCr, creatine plus phosphocreatine; tCho, glycerophosphocholine plus phosphocholine; tNAA, *N*-acetylaspartate plus *N*-acetylaspartylglutamate.

Grace Choi and Seungho Kim contributed equally to this work.

This is an open access article under the terms of the [Creative Commons Attribution-NonCommercial-NoDerivs](https://creativecommons.org/licenses/by-nc-nd/4.0/) License, which permits use and distribution in any medium, provided the original work is properly cited, the use is non-commercial and no modifications or adaptations are made.

© 2025 The Author(s). *NMR in Biomedicine* published by John Wiley & Sons Ltd.

1 | Introduction

Glutathione (GSH), a major antioxidant, plays an important role in protecting reactive molecules in living cells against oxidative stress [1]. Altered concentrations of GSH in the human brain have been reported in several neurological diseases such as cancer [2], schizophrenia [3], multiple sclerosis [4], Parkinson's disease [5], epilepsy [6], and Alzheimer's disease [7], as measured by proton MRS. The capability to measure the brain GSH level noninvasively and accurately by MRS is therefore of value clinically.

GSH is a tripeptide consisting of glycine, cysteine, and glutamate moieties and presents MR signals at many spectral locations [8]. All these GSH resonances appear in the proximity of abundant resonances of other brain metabolites, and as a result, none of the signals from this low-concentration metabolite are visually discernible in conventional MR spectra from the brain at the clinically popular field strength 3T or below. This spectral complexity is commonly overcome by means of spectral editing approaches incorporating the J-coupling features of the GSH spin system. Among many spectral editing approaches, J-difference spectroscopy (MEGA) [9] is well established and widely used to selectively detect the ~2.95 ppm resonance of the cysteine moiety, whereas the neighboring abundant total creatine (tCr) singlet (3.03 ppm) and the multiplet of γ -aminobutyric acid (3.01 ppm) are suppressed via subtraction between subsans [10, 11].

The proton spin resonances of the GSH cysteine moiety may be modeled by an ABX system with A, B, and X spins resonating at 2.93, 2.97, and 4.56 ppm, respectively, and scalarly coupled with strengths of $J_{AX} = 7.1$ Hz, $J_{BX} = 4.71$ Hz, and $J_{AB} = -14.1$ Hz [8]. In MEGA spectroscopy, when the 4.56-ppm resonance is selectively rotated through 180° in edit-on scans, the resulting positive signal of GSH at 2.95 ppm remains about the same with changing TE in a long- T_2 situation such as in an aqueous solution. As the GSH proton spins undergo ordinary J evolution during the edit-off sequence, the difference-edited GSH signal yield changes with the TE of the MEGA sequence. Because the edit-off signal of GSH is progressively inverted with increasing TE up to 140 - 150 ms, where the in-phase coherences of the CH_2 proton resonances are maximized with negative polarity, the difference-edited 2.95-ppm signal increases progressively with TE up to 130–140 ms. Many prior brain GSH measurements using MEGA MRS were performed with TEs longer than 100 ms [11–13], largely based on phantom observations.

Determination of an optimum TE of MEGA spectroscopy may require the T_2 of the target resonance in addition to the J-evolution effect. GSH is a large and heavy molecule (molecular weight of 307 g/mol). Compared with other brain metabolites, the proton spins of GSH may undergo much faster T_2 relaxation, as indicated in a prior GSH T_2 study at 4T (T_2 of 67 ms) [14]. There is a paucity in brain GSH T_2 measurements at 3T.

Designing MRS sequence parameters for maximum possible signal yield would be important for detecting a weak resonance. Sequence tailoring for maximizing the peak amplitude

may be preferable in MRS as it is directly relevant to the signal detectability and signal-to-noise ratio (SNR). The amplitude of a multiplet can be enhanced by manipulating the in-phase and antiphase coherence evolutions. In MEGA-PRESS, the timings of the spectrally selective editing pulses with respect to the second slice-selective 180° pulse provide an effective means to manipulate the coherence evolution during the edit-on sequence and eventually enhance the peak amplitude in difference spectra, as demonstrated in a recent lactate MEGA MRS study [15].

Here, we report evaluation of the GSH T_2 in the human brain at 3T, achieved with MEGA-PRESS at two sites with different vendors. Multiple TEs for T_2 evaluation are introduced incorporating optimized timings of the editing pulses. In addition to GSH T_2 evaluation, multi-TE spectral analysis is discussed for assessing the TE dependence of the difference-edited GSH signal detectability.

2 | Methods

T_2 evaluation of GSH in the human brain was performed with J-difference MRS at two sites, Vanderbilt University Medical Center (Site 1) and Kyungpook National University (Site 2). Proton MR experiments were carried out on a Philips 3-T scanner at Site 1 and on a GE 3-T scanner at Site 2 (Table 1). Human MR protocols were approved by the local Institutional Review Boards. Written informed consent was obtained from each subject prior to the MR scans.

Two 10-ms spectrally selective Gaussian editing 180° RF pulses, truncated at 7% (bandwidth 120 Hz), were implemented in the MEGA-PRESS sequences at the two sites (Figure 1A,B). The editing pulses were tuned at 4.56 ppm in edit-on scans and turned off in edit-off scans for editing of the GSH 2.95-ppm resonance. Single-voxel localization was obtained with vendor-supplied RF pulses (Figure 1C,D, and Table 1). The minimum TEs of the sequences at the two sites were both 58 ms for the given RF and gradient pulse durations.

Density-matrix simulations were carried out to determine the TEs for GSH T_2 evaluation and tailor the timings of the 10-ms editing pulses with respect to the second slice-selective 180° RF pulse (i.e., τ_1 and τ_2 in Figure 1A). The time evolution of the density operator during the sequence was numerically calculated using a product-operator-based transformation-matrix approach [16], programmed with Matlab (The MathWorks Inc.). Transformation matrices were created for the slice-selective 90° and 180° pulses, incorporating the actual slice-selective RF and gradient pulse envelopes, and used to calculate single-voxel localized MEGA spectra according to a published algorithm (Supplementary Methods) [17]. Spectra were calculated for a TE range of 58–160 ms with 1-ms increments and for all possible τ_1 and τ_2 values with 0.5-ms increments at individual TEs. The total number of timing sets, $(\text{TE}_1, \text{TE}_2, \tau_1, \tau_2)$, was 364,312, for each of which the edit-on, edit-off and difference spectra were calculated. For each TE, three sets of τ values were defined: (1) (τ_1, τ_2) of maximum GSH edited peak amplitude (optimum- τ), (2) maximum (τ_1, τ_2) values (maximum- τ), and (3) (τ_1, τ_2) satisfying $\tau_1 = \tau_2 = \text{TE}/4$ (quarter-TE τ). The GSH

TABLE 1 | MRI scanners and the parameters of slice-selective (SS) RF pulses and in vivo human brain MRS scans at Site 1 and Site 2.

Parameters	Site 1	Site 2
MRI vendor	Philips Elition 3T	GE Signa Architect 3T
RF transmission	Whole-body coil	Same as left
RF reception coil	32 channel coil	48 channel coil
SS90° pulse duration	7.1 ms	3.6 ms
SS90° pulse bandwidth	2.2 kHz	2.4 kHz
SS180° pulse duration	6.9 ms	8.0 ms
SS180° pulse bandwidth	1.3 kHz	2.6 kHz
SS pulse carrier frequency	3.0 ppm	2.7 ppm
Editing pulse duration	10 ms (Gaussian envelope)	Same as left
Editing pulse bandwidth	120 Hz	Same as left
Human subjects	5 healthy adults	Same as left
Age	25 ± 4 years	25 ± 2 years
Gender	2 male and 3 female	Same as left
Voxel size	25 × 30 × 30 mm ³	Same as left
TR	2 s	Same as left
TE	58, 70, 88, 116, and 150 ms	Same as left
Number of excitations	80 edit-on and 80 edit-off	Same as left
Sweep width	2500 Hz	5000 Hz
Number of sampling points	2048	4096
B0 shimming	Second order	First order
Hz/ppm	127.75	127.76

peak amplitude was calculated from spectra broadened to a singlet linewidth (FWHM) of 6 Hz (3-Hz exponential and 3-Hz Gaussian broadening).

Phantom MRS experiments were carried out using an aqueous solution with GSH 20 mM and glycine 30 mM at Site 1 and using a solution with GSH 20 mM and glycine 20 mM at Site 2. Both solutions were at neutral pH. Data were collected at five TEs (58, 70, 88, 116, and 150 ms), with TR 2 s, 16 excitations for each subscan, and voxel size of 25 × 25 × 25 mm³. The three τ schemes were tested at Site 1, but only the maximum- τ scheme was tested at Site 2 because the other two schemes were not available in the sequence implementation.

In vivo brain MRS data were collected from five healthy adult subjects at each site. The scan parameters are shown in Table 1. Data were acquired from 25 × 30 × 30 mm³ voxels in the medial posterior brain in individual subjects. Water suppression was obtained with variable flip-angle schemes [18, 19]. The editing pulse timings were set to the optimum- τ scheme at Site 1 and to the maximum- τ scheme at Site 2. Water-suppressed FIDs were recorded in multiple blocks. For Site 1, the editing pulse carrier frequency was switched in alternating blocks, each block having 16 averages of water-suppressed RF-phase-cycled FIDs. An unsuppressed water signal was acquired with

editing pulses turned off at the beginning of each block and used as reference in multichannel combination and eddy-current compensation. Frequency drifts were corrected real time in each excitation using a vendor-supplied tool. For Site 2, the edit-on and edit-off subscans were executed in alternate fashion and each FID was recorded separately. An unsuppressed water signal was acquired with editing pulses turned off at the beginning and used as reference in multichannel combination and eddy-current compensation. An eight-step phase cycling scheme was applied for each of edit-on and edit-off acquisitions.

The in vivo multiblock MEGA-PRESS data were frequency aligned and phase corrected prior to summation. Data were apodized with 1-Hz exponential and 1-Hz Gaussian functions before Fourier transformation. Spectral fitting of difference spectra was then performed with LCModel software [20] using an in-house basis set of 20 metabolites, which included GSH, *N*-acetylaspartate (NAA), NAA aspartate, *N*-acetylaspartateglutamate, creatine, phosphocreatine, phosphocholine, glycerophosphocholine, glutamate, glutamine, aspartate, taurine, myo-inositol, ethanolamine, phosphoethanolamine, glucose, lactate, threonine, and macromolecular species resonating at 1.42 and 1.24 ppm [21]. The LCModel built-in macromolecules and lipids bases were excluded in the fitting.

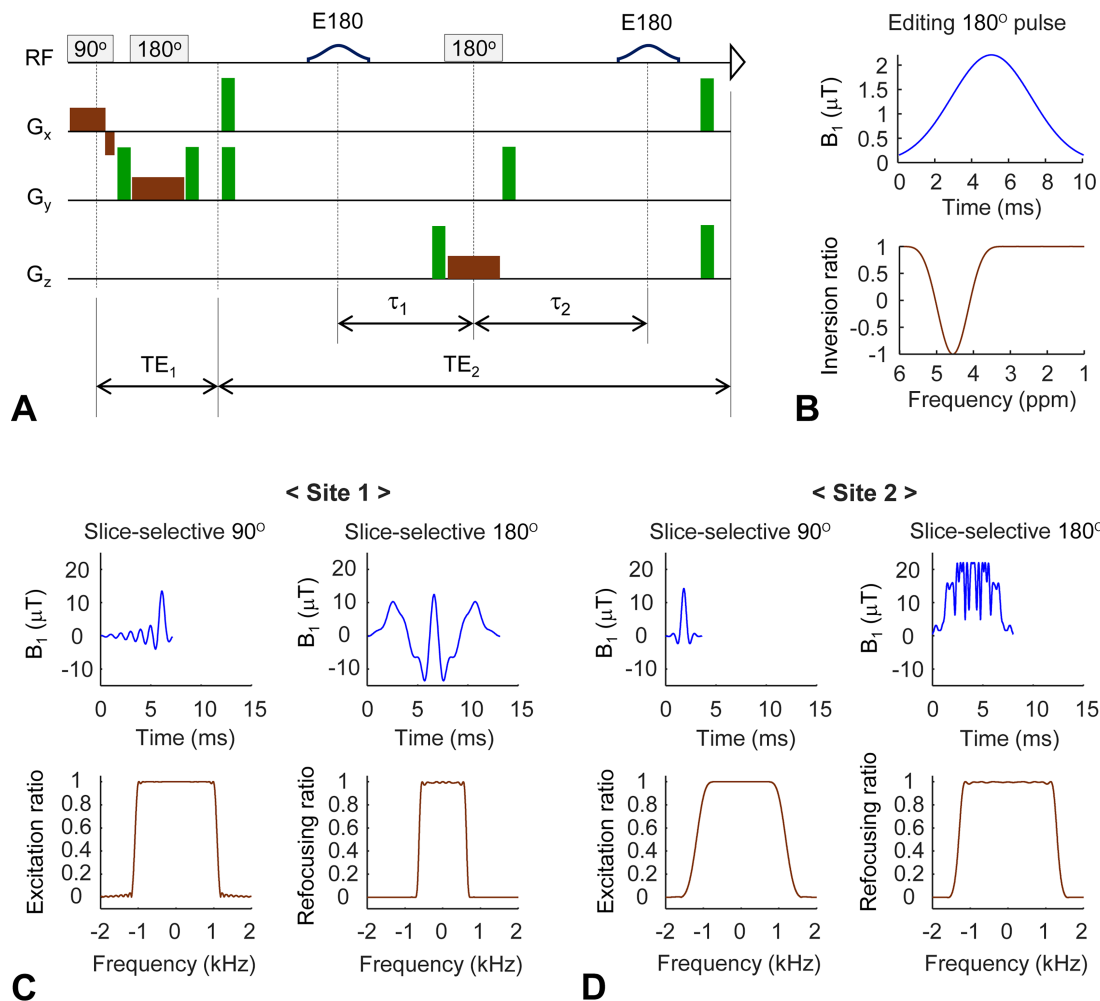


FIGURE 1 | (A) Schematic diagram of the single-voxel localized MEGA-PRESS sequence of the present study. The first subecho time TE_1 was 15 and 16 ms at Site 1 and Site 2, respectively. The TE_2 period had two editing 180° Gaussian pulses (E180) applied at time intervals τ_1 and τ_2 from the second slice-selective 180° pulse. Slice-selective gradients are shown in brown and spoiling gradients in green. (B) The envelope of the 10-ms Gaussian editing RF pulse (truncated at 7%) is shown together with the Bloch-simulated frequency profiles (120-Hz bandwidth at half amplitude). The editing pulses were set to 4.56 ppm in the edit-on scans and turned off in the edit-off scans. (C, D) The slice-selective 90° and 180° RF pulses used at Site 1 and Site 2 are shown together with Bloch-simulated frequency profiles. For Site 1, the 90° and 180° pulses were 7.1 and 6.9 ms long at B_1 of $13.5\mu\text{T}$ (both amplitude modulated), giving a 2.2-kHz excitation bandwidth and a 1.3-kHz refocusing bandwidth, respectively. For Site 2, the 90° and 180° pulses were 3.6 and 8.0 ms long, giving a 2.4-kHz excitation bandwidth ($B_1 = 14.3\mu\text{T}$) and a 2.6-kHz refocusing bandwidth ($B_1 = 22.0\mu\text{T}$), respectively. The 90° pulse was amplitude modulated and the 180° pulse was amplitude/frequency modulated. The frequency modulation of the 180° pulse is not shown for brevity.

Here, NAA denotes a singlet-only basis signal, which was included for fitting an artificial singlet that was added at 2.01 ppm in difference spectra to achieve proper phasing and frequency reference in LCModel fitting, similarly to a prior study [22]. In addition, LCModel fitting of edit-off spectra was performed using a metabolite basis set that additionally included γ -aminobutyric acid, glycine, and scyllo-inositol. The LCModel built-in macromolecular and lipid basis signals were included in the edit-off spectral fitting. The metabolite basis signals were prepared incorporating the actual slice-selective and spectrally selective RF and gradient pulse envelopes of the MEGA-PRESS sequences, according to a published simulation method [17]. Published chemical-shift and J-coupling constants were used in the simulations [8]. The spectral fitting was conducted between 0.2 and 4.0 ppm. The basis sets were generated at Site 1. LCModel fitting was carried out independently at the two sites.

GSH T_2 evaluation was performed with mono-exponential regression of LCModel estimates of the difference-edited signal at 2.95 ppm versus TE. A mono-exponential fitting was also undertaken on the co-edited NAA multiplet (aspartate moiety). LCModel signal estimates of tNAA and tCr from edit-off spectra were similarly analyzed. The T_2 relaxation-free estimation of GSH level was calculated with reference to zero-TE extrapolated tCr estimation at 8 mM [23, 24]. The Cramér-Rao lower bounds (CRLB) and correlation coefficients were returned by LCModel as percentage standard deviations of metabolite signal estimates and a measure of signal resolution, respectively. The contents of gray matter, white matter, and cerebrospinal fluids within the MRS voxels were estimated from segmentation of the T1-weighted images using FSL (FMRIB Software Library) [25] at Site 1 and SPM (Statistical Parametric Mapping) [26] at Site 2. Data are presented with mean \pm standard deviation.

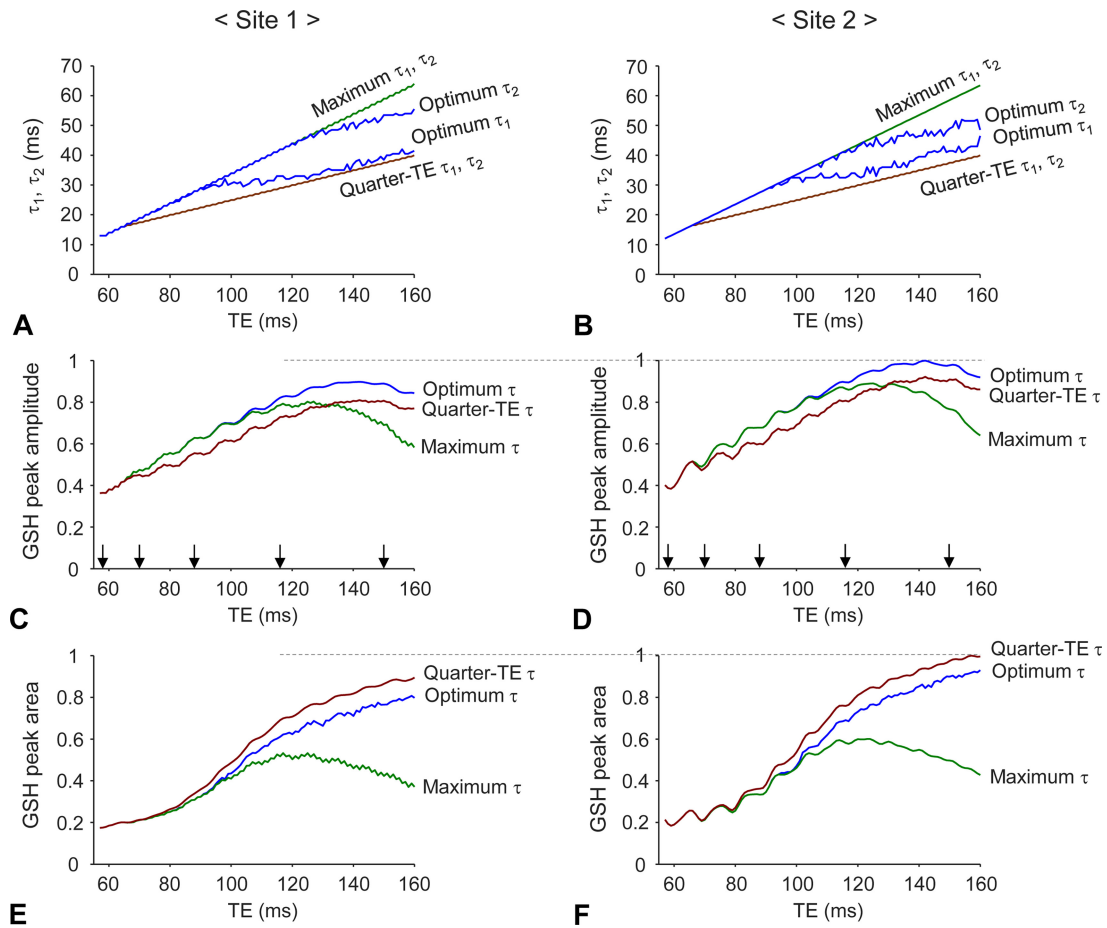


FIGURE 2 | (A,B) The τ_1 and τ_2 values are plotted versus TE for three schemes for Sites 1 and 2: (1) maximum possible τ_1 and τ_2 , (2) optimum τ_1 and τ_2 , and (3) quarter-TE τ_1 and τ_2 (satisfying $\tau_1 = \tau_2 = TE/4$). Here optimum τ_1 and τ_2 denote the τ values where the difference-edited GSH peak amplitude was calculated to be maximum in density-matrix simulations. (C,D) The calculated difference-edited GSH peak amplitude is plotted versus TE for the three τ schemes, ignoring T_2 relaxation effects. Five arrows indicate the TEs at which data were collected for GSH T_2 evaluation. (E,F) The calculated difference-edited GSH peak area is plotted versus TE for the three τ schemes, ignoring T_2 relaxation effects. In C–F, the peak amplitudes and areas were calculated from GSH signals broadened to singlet FWHM of 6 Hz. The peak area was obtained between 2.8 and 3.1 ppm.

3 | Results

Numerical simulations indicated that the MEGA-PRESS difference-edited GSH signal yield depends on the editing-pulse timings with respect to the second slice-selective 180° RF pulse. The difference-edited GSH 2.95-ppm peak amplitude exhibited a local maximum in the (τ_1, τ_2) plane for TEs between 58 and 160 ms (Figure S1). These maximum-amplitude, optimum τ_1 and τ_2 values increased with TE (Figure 2A,B). For relatively short TEs (< 95 ms), where τ_1 and τ_2 were not very changeable for given RF and gradient pulse durations, the optimum τ values were essentially identical to maximum- τ values. For the slice-selective RF pulses of both Site 1 and Site 2, the optimum τ_1 began to be smaller than the maximum τ_1 from TE 95 ms, and the optimum τ_2 became smaller than the maximum τ_2 from TE 120–130 ms. The calculated difference-edited GSH signal was clearly different between the three τ schemes. Ignoring the T_2 relaxation effect, the edited GSH peak amplitude from the optimum- τ set was maximum at TE 140, at which (τ_1, τ_2) equaled (37, 51) and (39.5, 46.5) ms for the Site-1 and Site-2 RF pulses, respectively (Figure 2C,D). The TE 140-ms peak amplitude at Site 1 was

predicted to be 90% with respect to that at Site 2, due largely to the difference in the slice-selective 180° RF pulse bandwidths used (1.3 vs. 2.6 kHz). The GSH peak amplitude of the maximum (τ_1, τ_2) sets dropped rapidly when TE exceeded 130 ms. The GSH peak height from the quarter-TE τ sets was overall lower compared with the optimum- τ scheme for the entire TE range studied. The quarter-TE τ scheme showed the largest peak area among the three τ schemes (Figure 2E,F), which was due to generation of large amounts of the GSH in-phase coherence following the quarter-TE τ sets. The peak area increased progressively with TE up to 160 ms. The calculated TE 160-ms peak area at Site 1 was 88% with respect to that at Site 2.

Phantom spectra of GSH and glycine are presented together with calculated spectra in Figure 3A. Whereas the edit-on GSH signal was positive across the five TEs, the edit-off GSH signal was somewhat positive at short TEs and inverted at long TEs, thereby resulting in a progressive increase of the difference-edited GSH signal with increasing TE. When a phantom T_2 of GSH was incorporated (350–400 ms), the simulated edit-on, edit-off, and difference-edited signals of GSH showed good

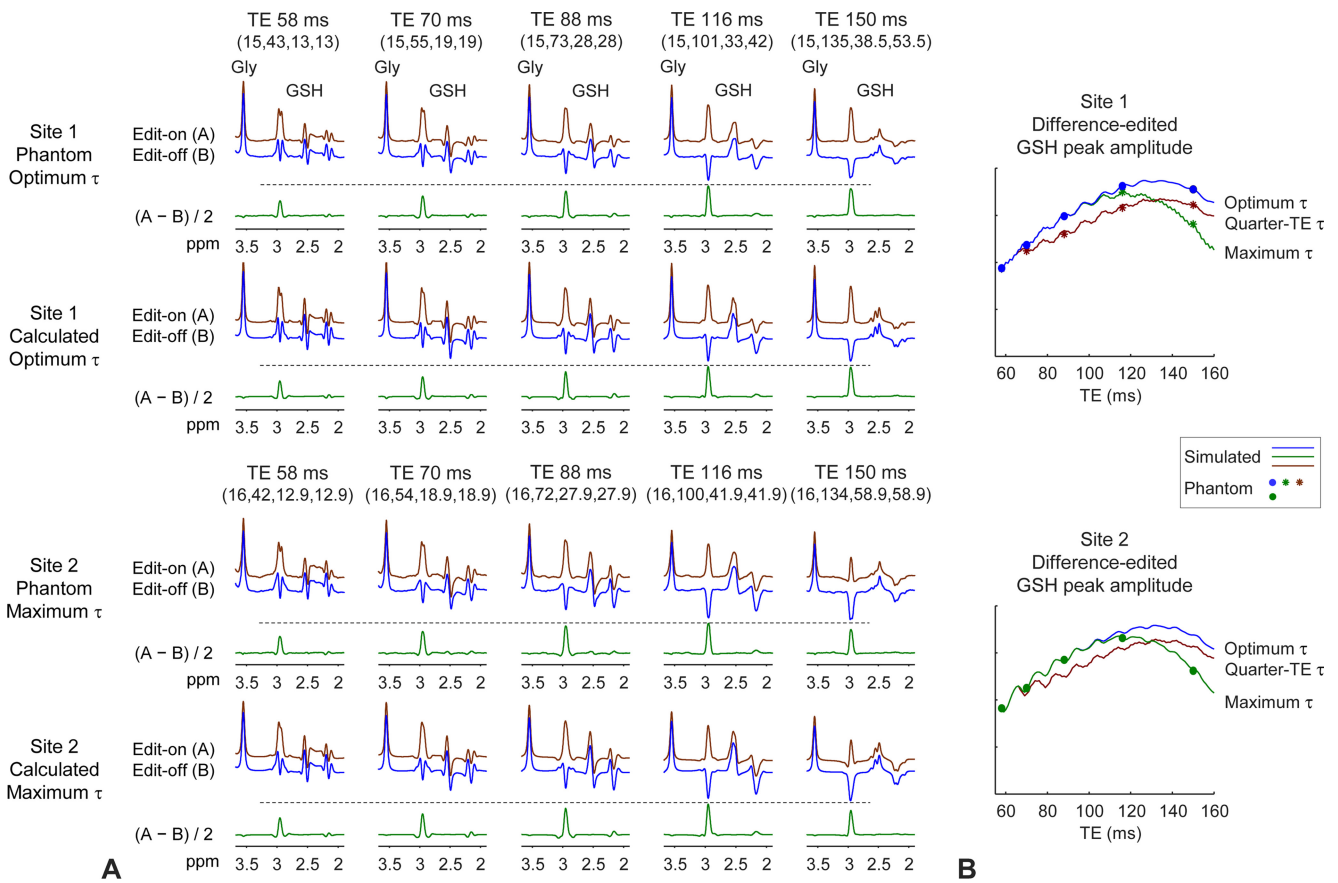


FIGURE 3 | (A) Phantom and numerically calculated MEGA-PRESS spectra of glycine and GSH are shown for five TEs (58, 70, 88, 116, and 150 ms) for Site 1 (upper panel) and Site 2 (lower panel). For individual TEs, the numbers in brackets are, from left to right, TE_1 , TE_2 , τ_1 , and τ_2 in milliseconds, where the τ_1 and τ_2 values at Site 1 were predicted to give maximum edited GSH peak amplitude (optimum τ_1 , τ_2) and those at Site 2 were maximum possible τ values. The spectra were broadened to glycine singlet FWHM of 6 Hz. The simulated spectra were adjusted with the experimental phantom T_2 values of glycine and GSH (900 and 400 ms for Site 1 and 850 and 350 ms for Site 2, respectively). (B) The calculated difference-edited GSH 2.95 ppm peak amplitude is plotted (solid lines) versus TE (58–160 ms, with 1-ms increments) for the three τ schemes for the MEGA-PRESS sequences of Site 1 and Site 2. Phantom GSH peak amplitudes, measured from the difference-edited spectra shown in A, are plotted (solid circles) on top of the simulated data (solid line). For Site 1, phantom GSH peak amplitude measurements using three other τ schemes are also presented.

agreement with phantom spectra for both sites. The difference-edited GSH peak amplitude was maximum between 125 and 130 ms for optimum- τ and quarter-TE τ sets (Figure 3B), whereas the maximum GSH peak amplitude of the maximum- τ scheme occurred at a shorter TE (~115 ms).

Figure 4 presents brain GSH T_2 data and voxel positioning in a subject at Site 1. The editing-pulse timings were set for maximum GSH peak amplitude (optimum- τ). With the use of 120 Hz bandwidth editing pulses tuned at 4.56 ppm in edit-on scans, the effects of the editing pulses on resonances up-field from 3.3 ppm were negligible (<0.1%), resulting in undetectable singlets of tCho, tCr (3.03 ppm), and tNAA in difference spectra. In addition to editing of the GSH 2.95 ppm resonance, the difference spectra showed co-edited signals of the creatine CH_2 resonance (3.92 ppm), NAA multiplet (2.4–2.8 ppm), lactate (1.31 ppm), threonine (1.32 ppm), and macromolecular species resonating at 1.42 and 1.24 ppm. The GSH signals at 2.95 ppm were well discernible in all difference spectra at the five TEs. The brain GSH signal at TE of 88 ms was larger than at other TEs, which was contrasted with the simulation and phantom data of optimum- τ sets (Figures 2C and 3B), where the GSH

signals at TEs of 116 and 150 ms were much larger than that at 58 ms TE (2.0–2.5 fold). Mono-exponential regression of the GSH signal estimates versus TE resulted in a T_2 of 88 ms in the subject. The T_2 of the co-edited NAA multiplet was measured as 238 ms. Monoexponential fitting of tCr and tNAA estimates from the edit-off spectra resulted in T_2 values of 149 and 240 ms, respectively.

In vivo data from a subject at Site 2 is presented in Figure 5. The editing-pulse timings were set to maximum- τ values. The TE dependences of edit-off and edit-on spectra were about the same as those at Site 1. Although the simulated GSH edited peak amplitude was much larger at 116 and 150 TEs compared with 58 ms TE (2.3 and 2.0 fold, respectively) (Figure 2D, green line), the brain GSH edited signal was the largest at TE of 88 ms. The ratios of the edited GSH and co-edited NAA signals to unedited singlets in edit-off spectra were overall larger compared with the data at Site 1, which was a benefit from the larger bandwidths of the slice-selective RF pulses at Site 2. Monoexponential regression of the GSH signal estimates versus TE resulted in a T_2 of 92 ms. The T_2 of the co-edited NAA multiplet was measured as 202 ms. Monoexponential fitting

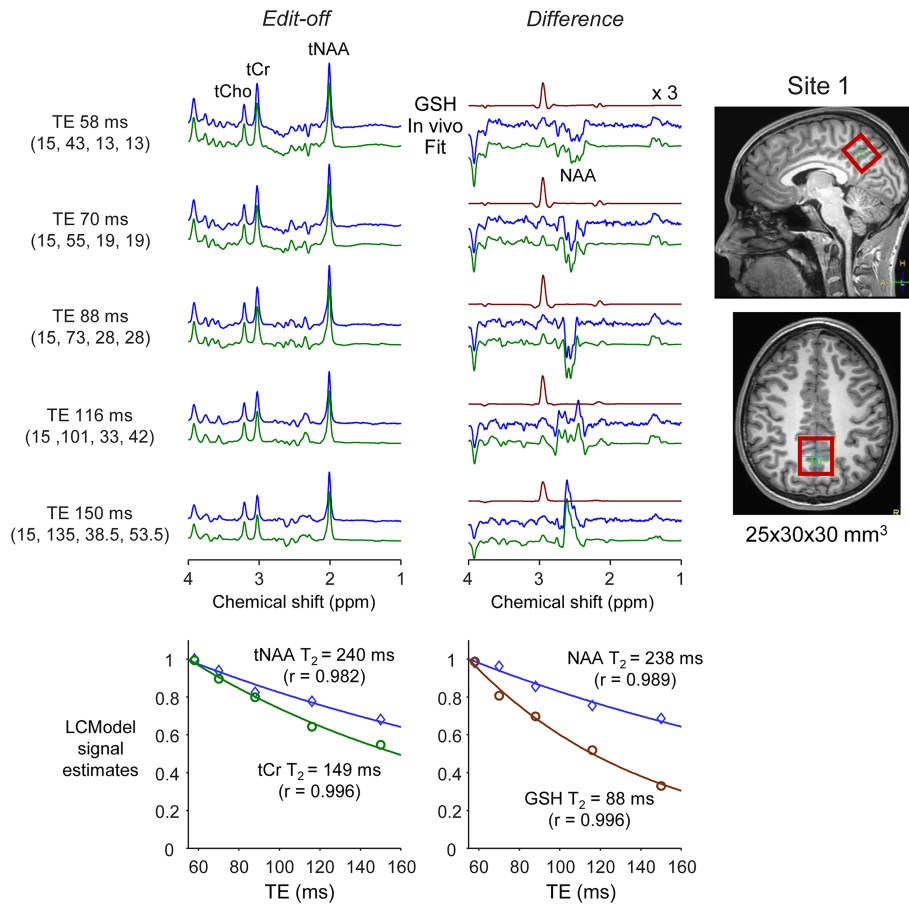


FIGURE 4 | (Upper panel) Representative in vivo MEGA-PRESS edit-off and difference spectra from a subject at Site 1, obtained at the five TEs, are presented together with LCMoel fits. The editing-pulse timings were set to optimum τ values. The LCMoel-returned GSH signals (in brown) were threefold magnified with respect to difference spectra that were fivefold magnified relative to edit-off spectra. The brain data were acquired with 80 averages for each of edit-on and edit-off scans at individual TEs (TR = 2s). (Lower panel) Monoexponential fitting of LCMoel estimates is presented for tNAA, tCr, NAA multiplet, and GSH. Here, the tNAA and tCr signals were estimated from edit-off spectra and the NAA multiplet and GSH signals from difference spectra. The voxel positioning ($25 \times 30 \times 30 \text{ mm}^3$) at Site 1 is shown on the right.

of tCr and tNAA estimates gave T_2 values of 131 and 221 ms, respectively.

MEGA-PRESS data were acquired from 10 subjects at two sites. Some data quality measures are presented for each site in Table 2. The FWHMs of water and tCr (3.03 ppm) peaks were measured to be slightly smaller at Site 1 than at Site 2, which may be due to the difference in B_0 shimming methods (i.e., second order vs. first order shimming). In contrast, the SNR of tCr, measured from edit-off spectra, was somewhat lower at Site 1 than at Site 2, which was due to the difference in actual localized volumes and number of channels in the receive coils between the sites. Although the bandwidth at half amplitude of the excitation and refocusing frequency profiles were used for determining the slice-selective gradient strengths at Site 2, the calculation of the slice-selective gradient strengths at Site 1 used the bandwidths of the excitation and refocusing frequency profiles at 10% levels, which was done to reduce outer-volume signals at the expense of reduction in SNR.

Figures 6 and 7 present in vivo difference spectra from five subjects respectively at Site 1 and Site 2, together with LCMoel

fits, LCMoel-returned GSH signals, and monoexponential fittings of the GSH and co-edited NAA multiplet estimates. A signal was visually discernible at 2.95 ppm in all spectra from the two sites. Brain GSH T_2 was estimated as 85 ± 8 and 90 ± 13 ms at Site 1 and Site 2, respectively (Table 2), without significant difference between the sites. The brain GSH T_2 estimate, averaged over the 10 subjects, was 88 ± 11 ms. Incorporating this GSH T_2 in the Figure 2C,D predicted that the maximum GSH edited peak amplitude would occur at TE < 100 ms for both sites (Figure S1). Normalizing the zero-TE extrapolated GSH estimates to the zero-TE tCr estimates and setting the tCr concentrations at 8 mM in individual subjects resulted in a brain GSH level of $1.6 \pm 0.2 \text{ mM}$ at Site 1 and $1.5 \pm 0.2 \text{ mM}$ at Site 2. The estimated GSH concentration was not significantly different between the sites. The zero-TE brain GSH concentration estimate averaged over the 10 subjects was $1.6 \pm 0.2 \text{ mM}$. The 95% confidence intervals of the GSH and NAA T_2 estimates and the correlation coefficients of the monoexponential fittings are shown in Table S1. The fractional gray matter, white matter, and cerebrospinal fluid contents within the MRS voxels were $47 \pm 3\%$, $37 \pm 2\%$, and $16 \pm 1\%$ for Site 1, and $65 \pm 2\%$, $24 \pm 2\%$, and $11 \pm 3\%$ for Site 2, respectively.

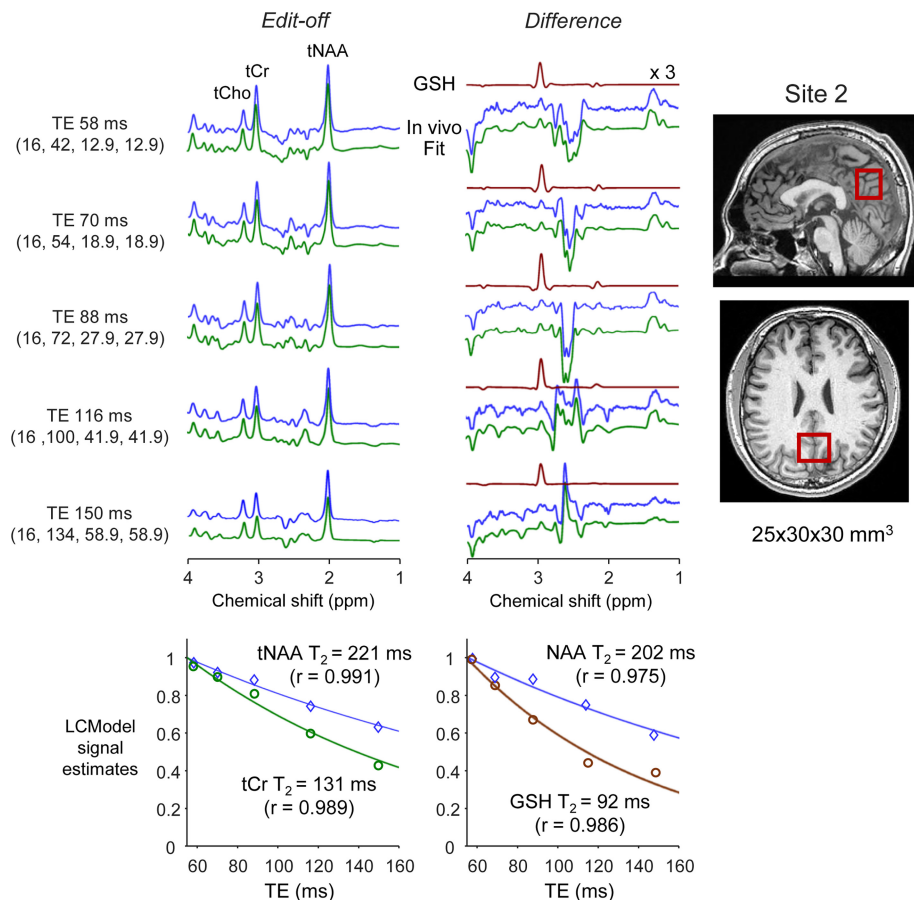


FIGURE 5 | Representative in vivo MEGA-PRESS edit-off and difference spectra from a subject and monoexponential fitting of LCMoel estimates of metabolite signals at Site 2 are presented in a similar fashion as in Figure 4.

TABLE 2 | In vivo brain MRS results from five subjects in each of Site 1 and Site 2. FWHM, SNR and CRLB were measured from 25 spectra for each site (five TEs in five subjects). Data are presented with mean \pm SD, where SD denotes the standard deviation across the measurements indicated by the sample size (N).

Quantity	Site 1	Site 2
Water FWHM ($N=25$)	6.4 \pm 0.4 Hz	7.2 \pm 0.5 Hz
tCr FWHM ($N=25$) ^a	6.0 \pm 0.2 Hz	6.8 \pm 0.4 Hz
tCr SNR ($N=25$)	132 \pm 12	106 \pm 34
GSH SNR ($N=25$) ^b	7.2 \pm 1.2	7.9 \pm 2.0
GSH CRLB ($N=25$) ^c	4.4 \pm 0.7%	5.7 \pm 1.8%
GSH T_2 ($N=5$)	85 \pm 8 ms	90 \pm 13 ms
tCr T_2 ($N=5$)	147 \pm 10 ms	140 \pm 10 ms
tNAA T_2 ($N=5$)	258 \pm 19 ms	229 \pm 7 ms
NAA multiplet T_2 ($N=5$)	227 \pm 18 ms	213 \pm 13 ms
tCr level ($N=5$)	8 mM	8 mM
GSH level ($N=5$)	1.6 \pm 0.2 mM	1.5 \pm 0.2 mM

^aMeasured from water-suppressed spectra apodized with a 1-Hz exponential and 1-Hz Gaussian function.

^bRatio of the LCMoel-returned GSH edited peak amplitude with respect to the LCMoel-returned residuals between 0.2 and 4.0 ppm.

^cThe LCMoel fitting was performed on spectra apodized with 1-Hz exponential and 1-Hz Gaussian functions.

For both sites, the mean CRLB over the five subjects showed slight differences between TEs (Table S2). The CRLB at TE of 88 ms was the smallest, which was likely because the in vivo detected GSH signal was larger at the TE than at other TEs. Because the edited GSH signal neighbors a large co-edited NAA multiplet in all difference spectra, we explored potential effects of the co-edited NAA multiplet on GSH signal estimation. LCMoel-returned correlations between the GSH and NAA multiplets exhibited negative values at short TEs (58, 70 and 88 ms) and positive values at long TEs (116 and 150 ms) (Table 3). The absolute values of the correlation coefficients were small at a TE of 58 ms and increased progressively with TE, indicating that the GSH signal can be better resolved from the co-edited NAA multiplet at short TEs.

4 | Discussion

The current study reports a multisite multivendor evaluation of the T_2 relaxation time and T_2 relaxation-free estimation of GSH in the human brain at 3 T in vivo. The signal intensity and spectral pattern of J-coupled spin metabolites vary with changing TE due to the combined effects of J evolution and T_2 relaxation. Thus, when basis spectra that include the J evolution effects only are used for spectral fitting of multi-TE data, the T_2 relaxation effect on the J-coupled spin signals can be assessed from the TE dependence of the integrated signal estimates. The effects of the

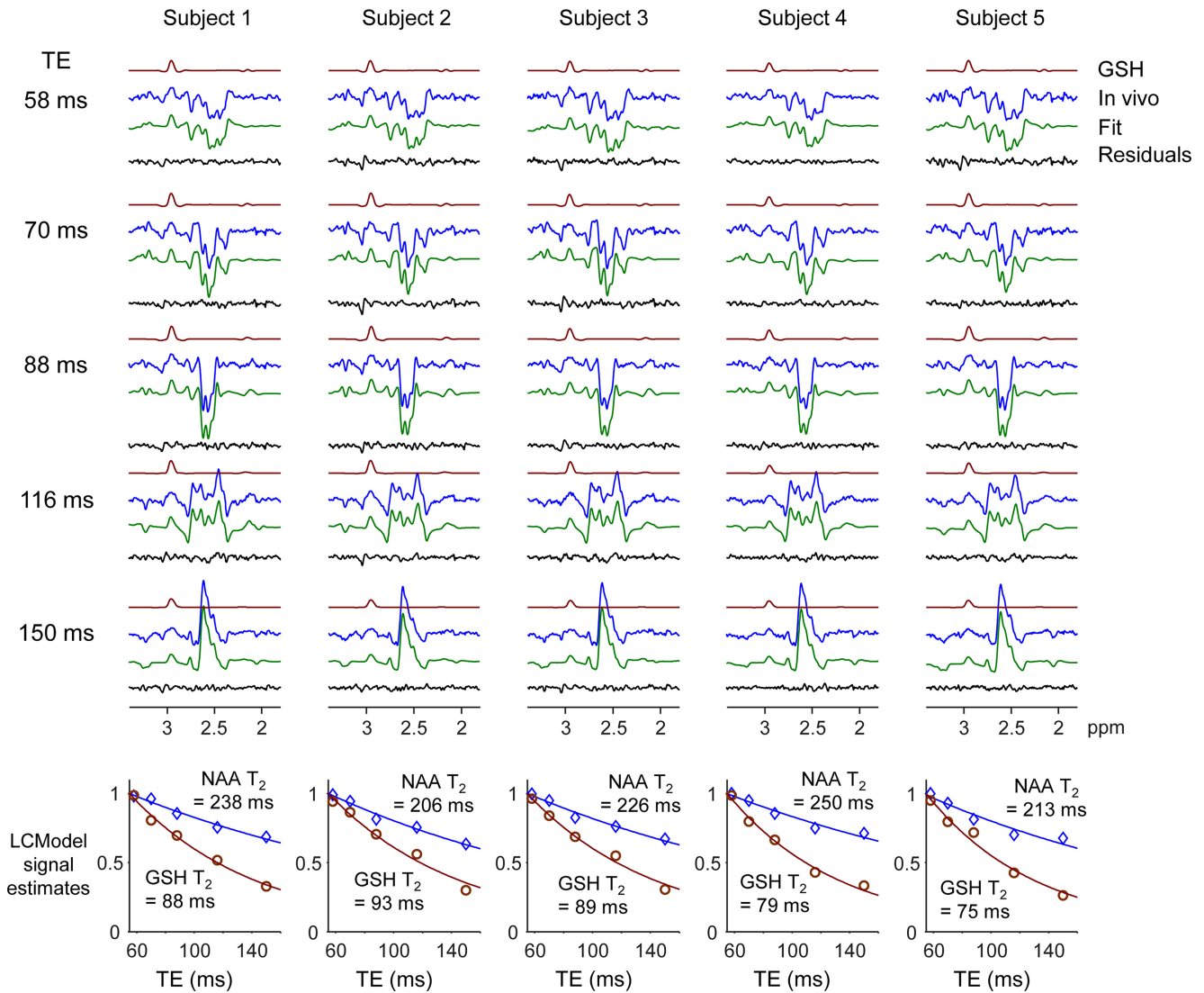


FIGURE 6 | Difference spectra from five subjects, obtained at Site 1, are presented together with LCModel-returned GSH signal, fits, and residuals in the upper panel. The monoexponential fittings of GSH and NAA multiplet in individual subjects are shown in the lower panel. The editing-pulse timings were set to optimum τ values at individual TEs. The estimated T_2 values of GSH and NAA multiplet are shown for each subject.

finite bandwidth and the resulting chemical-shift associated voxel displacements need to be considered in measuring the signals, which was addressed in the present study.

The T_2 estimates at two sites with different vendors were not significantly different from each other, and the brain GSH T_2 estimate from combining the data from the sites was 88 ± 11 ms ($N=10$). Also, the GSH concentration, estimated from the zero-TE extrapolated signal strength, was not significantly different between the sites. The brain GSH level was measured as 1.6 ± 0.2 mM ($N=10$) with reference to tCr at 8 mM, overall larger compared with prior GSH reports (0.8–1.9 mM) [10, 12–14, 27]. Our GSH T_2 estimate at 3T may be in reasonable agreement with a prior brain GSH T_2 measure at 4T (67 ms) [14], considering that the T_2 relaxation time is expected to decrease with increasing field strength. A 3-T 2D-MRS study reported T_2 values of 17 brain metabolites including GSH [28].

The TE range of the present study is relatively small compared with prior T_2 studies in other metabolites at 3T [29–32], whose T_2

values are relatively long (> 150 ms). A short editing pulse (10 ms) having negligible effects on the GSH 2.95 ppm resonance when tuned at 4.56 ppm was employed in the present study, thereby maximizing the TE range and consequently the dynamic range of the signal variations. It is noteworthy that our 92 ms TE range (58–150 ms) is much larger than the TE range (102–152 ms) of the prior GSH T_2 study at 4T [14]. Given that J-evolution causes the GSH edited signal to rapidly drop at TEs > 150 ms, including very long TEs in GSH T_2 evaluation may not be realistic. The TE range we opted for would be reasonable for evaluating the relatively short T_2 of GSH at 3T.

It appears that the GSH edited signal differences between the three τ schemes are the consequences of differential coherence evolutions during the MEGA-PRESS sequence. For an ABX spin system of the GSH cysteine moiety, following a 90° excitation of the thermal equilibrium, the in-phase coherences of A and B spins undergo J evolution during the sequence, and the GSH signal at 2.95 ppm may be largely determined by four in-phase coherences (i.e., A_y , B_y , A_x , and B_x) and four antiphase coherences

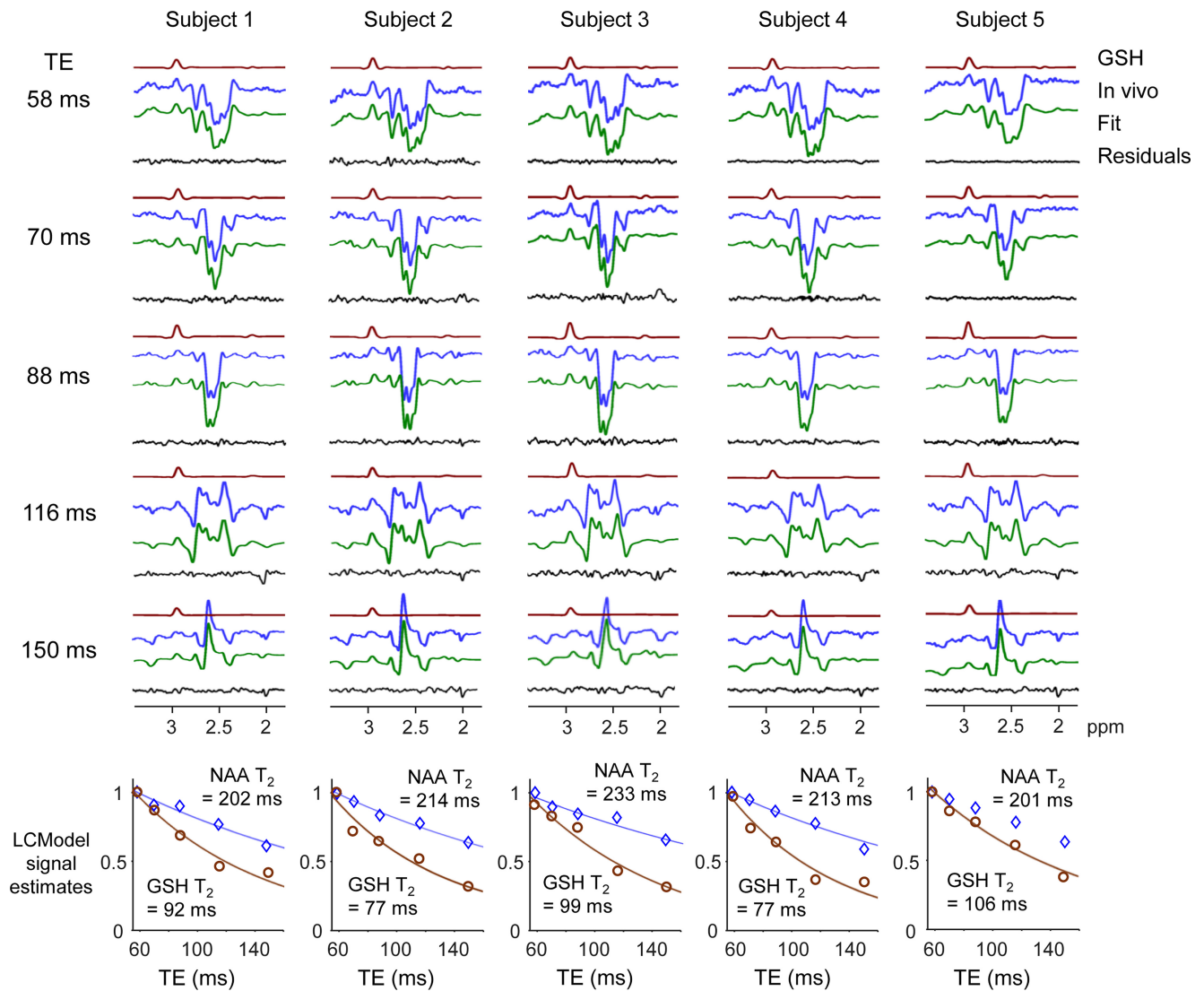


FIGURE 7 | Difference spectra from five subjects, obtained at Site 2, are presented together with monoexponential fittings of GSH and NAA multiplet in a similar fashion as in Figure 6. The editing-pulse timings were set to maximum τ values at individual TEs.

(i.e., $2A_xX_z$, $2B_xX_z$, $2A_yX_z$, and $2B_yX_z$) at the onset of the FID acquisition (Figure S3). For an edit-off scan, the GSH 2.95 ppm signal is small and partially positive at $TE < 100$ ms due to co-presence of many in-phase and antiphase coherences, and at $TE > 100$ ms the in-phase coherences, A_y and B_y , which give an inverted signal at 2.95 ppm, are predominant in signal formation. In contrast, the edit-on scans maintain the production of the $-A_y$ and $-B_y$ coherences with changing TE, giving a positive in-phase signal at 2.95 ppm. A major difference between the three τ schemes is in production of $-2A_xX_z$, $-2B_xX_z$, both of which give rise to a narrow positive peak at 2.95 ppm. Although the production of these antiphase coherences is minimal in quarter-TE τ sets, the coherences are largely generated in the optimum- τ and maximum- τ schemes. It is worthwhile to note that, in MEGA-PRESS scans with optimum- τ sets, the antiphase coherences ($-2A_xX_z$, $-2B_xX_z$) and the in-phase coherences ($-A_y$ and $-B_y$) additively contribute to signal formation, thereby leading to high and narrow GSH peaks at 2.95 ppm.

Although production of a high and narrow peak may be generally favorable for detecting a weak resonance, the reliability and

precision in estimating a signal strength are largely governed by potential interferences of adjacent abundant resonances. The signal resolution and detectability can be assessed with the correlation coefficients returned by LCMoDel. Among the five TEs of the present study, the correlation coefficient between GSH and the co-edited NAA multiplet was clearly smaller at short TEs than at long TEs. This is most likely due to the difference in the co-edited NAA signal polarity in the proximity of 2.95 ppm. The co-edited NAA multiplets at short TEs have relatively small signal tails with positive polarity at ~ 2.9 ppm, whereas the multiplets at long TEs exhibit non-negligible negative signals near the GSH resonance. It appears that MEGA-PRESS GSH estimation with minimum interferences is achievable at short TEs, although the edited GSH signal intensity is somewhat low and thus the CRLB is large.

Some limitations are present in the current study. First, the small sample size is a major pitfall. Our findings may require validation in a larger number of subjects to have sufficient statistical power although the result was obtained from multiple sites and multiple vendors. Second, the GSH T_2 estimated in this

TABLE 3 | LCModel-returned correlation coefficients between MEGA-edited GSH and NAA multiplets are tabulated for the five TEs used for T_2 evaluation.

Site 1						
TE (ms)	Subject 1	Subject 2	Subject 3	Subject 4	Subject 5	Mean \pm SD
58	-0.006	-0.009	-0.003	-0.011	-0.007	-0.0072 \pm 0.0030
70	-0.013	-0.05	-0.037	-0.058	-0.012	-0.0340 \pm 0.0210
88	-0.099	-0.065	-0.073	-0.053	-0.047	-0.0674 \pm 0.0204
116	0.071	0.072	0.067	0.082	0.084	0.0752 \pm 0.0074
150	0.068	0.094	0.073	0.079	0.109	0.0846 \pm 0.0168
Site 2						
TE (ms)	Subject 1	Subject 2	Subject 3	Subject 4	Subject 5	Mean \pm SD
58	-0.02	-0.083	-0.009	-0.051	-0.074	-0.0474 \pm 0.0325
70	-0.011	-0.063	-0.038	-0.113	-0.056	-0.0562 \pm 0.0376
88	-0.023	-0.064	-0.092	-0.069	-0.074	-0.0644 \pm 0.0254
116	0.042	0.129	0.138	0.132	0.038	0.0958 \pm 0.0511
150	0.138	0.174	0.159	0.107	0.056	0.1268 \pm 0.0469

study should be taken as an apparent transverse signal decaying rate occurring in a PRESS-type of MRS sequences, which may include molecular diffusion effects in the human brain [33]. Lastly, given that prior studies reported unequal T_2 values and concentrations of well-measurable metabolites between brain regions [29–31], our GSH T_2 and T_2 relaxation-free estimation of GSH may be applicable to the brain region and volume of the present study.

5 | Conclusions

We report the first evaluation of apparent T_2 relaxation and T_2 relaxation-free estimation of GSH in the human brain at 3T, achieved with MEGA-PRESS. The brain GSH T_2 estimate (88 \pm 11 ms) was shorter by twofold or more compared with other well-detectable metabolites. The brain GSH concentration, calculated from the zero-TE extrapolated magnetization, was 1.6 \pm 0.2 mM with reference to tCr at 8 mM. It follows that, with the effect of the fast T_2 relaxation, the brain GSH MEGA-PRESS signal may be maximized at TEs shorter than 100 ms, with dependence on other sequence parameters such as the duration and timings of editing RF pulses. Short TEs may be favorable for resolving the difference-edited GSH signal from the co-edited NAA multiplet with high confidence. Further studies are required to determine variations in GSH T_2 and GSH concentrations across brain regions, between gray and white matter, and during disease.

Acknowledgments

This research was supported by a National Research Foundation of Korea (NRF) grant funded by the Korea government (MSIT) (No. RS-2024-00406209) and the National Institutes of Health (Grant No.: S10OD021771-01 and UL1TR002243). We acknowledge institutional

funds provided by VICC, VUIIS, and the Departments of Radiology and Radiological Sciences and Neurological Surgery of Vanderbilt University Medical Center.

Conflicts of Interest

R.N. is an employee of GE Healthcare and has no competing interests. R.K.R. is an employee of Philips and has no competing interests.

Data Availability Statement

The data that support the findings of this study are available on request from the corresponding author. The data are not publicly available because of privacy or ethical restrictions.

References

1. R. Dringen, "Metabolism and Functions of Glutathione in Brain," *Progress in Neurobiology* 62 (2000): 649–671.
2. K. S. Opstad, S. W. Provencher, B. A. Bell, J. R. Griffiths, and F. A. Howe, "Detection of Elevated Glutathione in Meningiomas by Quantitative in Vivo ^1H MRS," *Magnetic Resonance in Medicine* 49 (2003): 632–637.
3. S. Lavoie, M. M. Murray, P. Deppen, et al., "Glutathione Precursor, N-Acetyl-Cysteine, Improves Mismatch Negativity in Schizophrenia Patients," *Neuropsychopharmacology* 33 (2008): 2187–2199.
4. H. Prinsen, R. A. de Graaf, G. F. Mason, D. Pelletier, and C. Juchem, "Reproducibility Measurement of Glutathione, GABA, and Glutamate: Towards in Vivo Neurochemical Profiling of Multiple Sclerosis With MR Spectroscopy at 7T," *Journal of Magnetic Resonance Imaging* 45 (2017): 187–198.
5. L. D. Coles, P. J. Tuite, G. Oz, et al., "Repeated-Dose Oral N-Acetylcysteine in Parkinson's Disease: Pharmacokinetics and Effect on Brain Glutathione and Oxidative Stress," *Journal of Clinical Pharmacology* 58 (2018): 158–167.
6. O. M. Gonen, B. A. Moffat, P. M. Desmond, E. Lui, P. Kwan, and T. J. O'Brien, "Seven-Tesla Quantitative Magnetic Resonance Spectroscopy of Glutamate, Gamma-Aminobutyric Acid, and Glutathione in the

- Posterior Cingulate Cortex/Precuneus in Patients With Epilepsy,” *Epilepsia* 61 (2020): 2785–2794.
7. P. K. Mandal, D. Dwivedi, S. Joon, et al., “Quantitation of Brain and Blood Glutathione and Iron in Healthy Age Groups Using Biophysical and In Vivo MR Spectroscopy: Potential Clinical Application,” *ACS Chemical Neuroscience* 14 (2023): 2375–2384.
8. V. Govind, “¹H-NMR Chemical Shifts and Coupling Constants for Brain Metabolites,” *eMagRes* 5 (2016): 1347–1362.
9. M. Mescher, H. Merkle, J. Kirsch, M. Garwood, and R. Gruetter, “Simultaneous in Vivo Spectral Editing and Water Suppression,” *NMR in Biomedicine* 11 (1998): 266–272.
10. M. Terpstra, P. G. Henry, and R. Gruetter, “Measurement of Reduced Glutathione (GSH) in Human Brain Using LCModel Analysis of Difference-Edited Spectra,” *Magnetic Resonance in Medicine* 50 (2003): 19–23.
11. F. Bottino, M. Lucignani, A. Napolitano, et al., “In Vivo Brain GSH: MRS Methods and Clinical Applications,” *Antioxidants (Basel)* 10 (2021): 1407.
12. L. An, Y. Zhang, D. M. Thomasson, et al., “Measurement of Glutathione in Normal Volunteers and Stroke Patients at 3T Using J-Difference Spectroscopy With Minimized Subtraction Errors,” *Journal of Magnetic Resonance Imaging* 30 (2009): 263–270.
13. F. Sanaei Nezhad, A. Anton, L. M. Parkes, B. Deakin, and S. R. Williams, “Quantification of Glutathione in the Human Brain by MR Spectroscopy at 3 Tesla: Comparison of PRESS and MEGA-PRESS,” *Magnetic Resonance in Medicine* 78 (2017): 1257–1266.
14. U. E. Emir, D. Deelchand, P. G. Henry, and M. Terpstra, “Noninvasive Quantification of T_2 and Concentrations of Ascorbate and Glutathione in the Human Brain From the Same Double-Edited Spectra,” *NMR in Biomedicine* 24 (2011): 263–269.
15. S. K. Ganji, Z. An, V. Tiwari, et al., “Optimization of Spectrally Selective 180 Degrees Radiofrequency Pulse Timings in J-Difference Editing (MEGA) of Lactate,” *Magnetic Resonance in Medicine* 87 (2022): 1150–1164.
16. R. B. Thompson and P. S. Allen, “Sources of Variability in the Response of Coupled Spins to the PRESS Sequence and Their Potential Impact on Metabolite Quantification,” *Magnetic Resonance in Medicine* 41 (1999): 1162–1169.
17. C. Choi, S. K. Ganji, R. J. Deberardinis, et al., “2-Hydroxyglutarate Detection by Magnetic Resonance Spectroscopy in IDH-Mutated Patients With Gliomas,” *Nature Medicine* 18 (2012): 624–629.
18. R. J. Ogg, P. B. Kingsley, and J. S. Taylor, “WET, a T1- and B1-Insensitive Water-Suppression Method for In Vivo Localized ¹H NMR Spectroscopy,” *Journal of Magnetic Resonance. Series B* 104 (1994): 1–10.
19. A. Haase, J. Frahm, W. Hanicke, and D. Matthaei, “¹H NMR Chemical Shift Selective (CHESS) Imaging,” *Physics in Medicine and Biology* 30 (1985): 341–344.
20. S. W. Provencher, “Estimation of Metabolite Concentrations From Localized In Vivo Proton NMR Spectra,” *Magnetic Resonance in Medicine* 30 (1993): 672–679.
21. K. L. Behar, D. L. Rothman, D. D. Spencer, and O. A. Petroff, “Analysis of Macromolecule Resonances in ¹H NMR Spectra of Human Brain,” *Magnetic Resonance in Medicine* 32 (1994): 294–302.
22. R. K. Robison, J. R. Haynes, S. K. Ganji, et al., “J-Difference Editing (MEGA) of Lactate in the Human Brain at 3T,” *Magnetic Resonance in Medicine* 90 (2023): 852–862.
23. R. Mekte, V. Mlynarik, G. Gambarota, M. Hergt, G. Krueger, and R. Gruetter, “MR Spectroscopy of the Human Brain With Enhanced Signal Intensity at Ultrashort Echo Times on a Clinical Platform at 3T and 7T,” *Magnetic Resonance in Medicine* 61 (2009): 1279–1285.
24. I. Tkac, G. Oz, G. Adriany, K. Ugurbil, and R. Gruetter, “In Vivo ¹H NMR Spectroscopy of the Human Brain at High Magnetic Fields: Metabolite Quantification at 4T vs. 7T,” *Magnetic Resonance in Medicine* 62 (2009): 868–879.
25. Y. Zhang, M. Brady, and S. Smith, “Segmentation of Brain MR Images Through a Hidden Markov Random Field Model and the Expectation-Maximization Algorithm,” *IEEE Transactions on Medical Imaging* 20 (2001): 45–57.
26. K. J. Friston, J. T. Ashburner, S. J. Kiebel, T. E. Nichols, and W. D. Penny, *Statistical Parametric Mapping: The Analysis of Functional Brain Images*, 1st ed., (London: Academic Press, 2006).
27. T. Satoh and Y. Yoshioka, “Contribution of Reduced and Oxidized Glutathione to Signals Detected by Magnetic Resonance Spectroscopy as Indicators of Local Brain Redox State,” *Neuroscience Research* 55 (2006): 34–39.
28. P. O. Wyss, C. Bianchini, M. Scheidegger, et al., “In Vivo Estimation of Transverse Relaxation Time Constant (T_2) of 17 Human Brain Metabolites at 3T,” *Magnetic Resonance in Medicine* 80 (2018): 452–461.
29. V. Mlynarik, S. Gruber, and E. Moser, “Proton T_1 and T_2 Relaxation Times of Human Brain Metabolites at 3 Tesla,” *NMR in Biomedicine* 14 (2001): 325–331.
30. F. Traber, W. Block, R. Lamerichs, J. Gieseke, and H. H. Schild, “¹H Metabolite Relaxation Times at 3.0 Tesla: Measurements of T_1 and T_2 Values in Normal Brain and Determination of Regional Differences in Transverse Relaxation,” *Journal of Magnetic Resonance Imaging* 19 (2004): 537–545.
31. C. Choi, N. J. Coupland, P. P. Bhardwaj, et al., “ T_2 Measurement and Quantification of Glutamate in Human Brain in Vivo,” *Magnetic Resonance in Medicine* 56 (2006): 971–977.
32. S. K. Ganji, A. Banerjee, A. M. Patel, et al., “ T_2 Measurement of J-Coupled Metabolites in the Human Brain at 3T,” *NMR in Biomedicine* 25 (2012): 523–529.
33. S. Michaeli, M. Garwood, X. H. Zhu, et al., “Proton T_2 Relaxation Study of Water, N-Acetylaspartate, and Creatine in Human Brain Using Hahn and Carr-Purcell Spin Echoes at 4T and 7T,” *Magnetic Resonance in Medicine* 47 (2002): 629–633.

Supporting Information

Additional supporting information can be found online in the Supporting Information section.